

Kinetics of Actin Unfolding Induced by Guanidine Hydrochloride[†]Konstantin K. Turoverov,[‡] Vladislav V. Verkhusha,^{§,||} Mikhail M. Shavlovsky,[‡] Alexander G. Biktashev,[‡] Olga I. Povarova,[‡] and Irina M. Kuznetsova^{*,‡}

Institute of Cytology, Russian Academy of Science, St. Petersburg 194064, Russia, Center for Molecular Medicine, Moscow University, Moscow 119899, Russia, and Institute for Experimental Medicine, Russian Academy of Medical Science, St. Petersburg 197376, Russia

Received June 1, 2001; Revised Manuscript Received October 10, 2001

ABSTRACT: The kinetics of actin unfolding induced by guanidine hydrochloride has been studied. On the basis of obtained experimental data a new kinetic pathway of actin unfolding was proposed. We have shown that the transition from native to inactivated actin induced by guanidine hydrochloride (GdnHCl) passes through essential unfolding of the protein. This means that inactivated actin should be considered as the off-pathway species rather than an intermediate conformation between native and completely unfolded states of actin, as has been assumed earlier. The rate constants of the transitions that give rise to the inactivated actin were determined. At 1.0–2.0 M GdnHCl the value of the rate constant of the transition from native to essentially unfolded actin exceeds that of the following step of inactivated actin formation. It leads to the accumulation of essentially unfolded macromolecules early in the unfolding process, which in turn causes the minimum in the time dependencies of tryptophan fluorescence intensity, parameter *A*, characterizing the intrinsic fluorescence spectrum position, and tryptophan fluorescence anisotropy.

Protein folding and refolding is often accompanied by the association of the partially folded intermediates (1–8). Protein association or aggregation represents an essential problem in biotechnology as overexpression of recombinant proteins is often complicated by the formation of the misfolded protein accumulated in inclusion bodies (9–15). The association of specific proteins and deposition of insoluble protein fibrils (amyloid) in various organs result in the development of many disorders such as Alzheimer's and Parkinson's diseases, malignant myeloma, cataracts, prion afflictions, and many other abnormalities (7, 16–25). The crucial importance of protein aggregation originating from partially folded species gave rise of a great number of studies considering this problem (see, e.g., ref 7).

Actin, one of the major proteins of muscle tissue, is a globular protein with a molecular mass of 42 kDa that is known to bind one divalent ion, Ca²⁺, and one molecule of ATP. Actin contains four tryptophan residues (26). Only two of these tryptophan residues, Trp 340 and Trp 356, which are localized in the hydrophobic environment, give essential contribution to actin intrinsic fluorescence (27, 28). At low ionic strength actin exists as a monomer (G-actin), but in the presence of neutral salts it is polymerized into a double-stranded polymer, which is known as the fibrous form of actin, or F-actin.

The release of calcium ion by EDTA or EGTA treatment leads to the transformation of G-actin into the inactivated form (I), in which the protein molecule loses its capability to polymerize (29, 30). Inactivated actin also may be obtained as a result of heat denaturation (29–41), moderate urea or GdnHCl¹ concentration (30, 38), dialysis from 8 M urea or 6 M GdnHCl (38, 39), or spontaneously during storage (38). Properties of inactivated actin are invariant to the way of denaturation (30, 42, 43). It also has been shown that inactivated actin is a thermodynamically stable monodisperse associate, consisting of 15 monomers (43). It has a unique structure, with hydrophobic clusters on the surface and polar regions in the interior (30, 42, 43). Thus inactivated actin represents an interesting system for the investigation of different aspects connected with the self-association of partially folded proteins.

In this work we focused on the process of the formation of inactivated actin. To elucidate the mechanism of inactivated actin formation, the kinetics of GdnHCl-induced actin unfolding was studied. It was shown that the essential unfolding of the protein macromolecule precedes the formation of inactivated actin.

MATERIALS AND METHODS

Preparations. Rabbit skeletal muscle actin was purified by the standard procedure (44). G-actin in buffer G (0.2 mM ATP, 0.1 mM CaCl₂, 0.4 mM β-mercaptoethanol, 5 mM Tris-HCl, pH 8.2, and 1 mM NaN₃) was stored on ice and used within 1 week. Actin was purified by one or two cycles of polymerization–depolymerization using 30 mM KCl for polymerization. Actin samples with the *A* parameter not

[†] This work was supported by Grants 00-04-49224, 00-04-81082, and 01-04-49308 from the Russian Foundation of Basic Research and St. Petersburg United Research Center (Joint Use Center), Russia.

* To whom correspondence should be addressed. Fax: 7(812)247-0341. E-mail: kkt@mail.cytspb.rssi.ru.

[‡] Institute of Cytology, Russian Academy of Science.

[§] Center for Molecular Medicine, Moscow University.

^{||} Current address: Tsukita Cell Axis Project, Kyoto Research Park, Shimogyo-ku, Kyoto 600-8813, Japan.

¹ Institute for Experimental Medicine, Russian Academy of Medical Science.

¹ Abbreviations: CD, circular dichroism; UV, ultraviolet; GdnHCl, guanidine hydrochloride; N, native; U, unfolded; I, inactivated actin.

lower than 2.56, which corresponds to the content of inactivated actin not higher than 2% (45), were used. Actin concentration was determined with a spectrophotometer (Hitachi, Japan). The molar extinction constant for actin was taken as $E_{280} = 1.09 \text{ mg mL}^{-1} \text{ cm}^{-1}$ (46). Actin concentration was varied from 0.01 to 0.1 mg/mL. GdnHCl (Nacalai Tesque, Japan) was used without additional purification. The concentration of GdnHCl was determined by the refraction index with an Abbe refractometer (LOMO, Russia). In the experiments of refolding the appropriate concentrations of GdnHCl were obtained by dilution of actin solution in 5 M GdnHCl.

Fluorescence Measurements. Fluorescence experiments were carried out using the spectrofluorimeter with steady-state excitation (47). Fluorescence was excited at the long-wave absorption edge where the contribution of tyrosine residues is negligible. The position and form of the fluorescence spectra were characterized by the parameter $A = (I_{320}/I_{365})_{297}$, where I_{320} and I_{365} are fluorescence intensities at $\lambda_{em} = 320$ and 365 nm, respectively, and $\lambda_{ex} = 297$ nm (47). In some cases the whole spectrum was recorded. The values of parameter A and of the fluorescence spectrum were corrected by the instrument sensitivity.

Vertical (I_V^V) and horizontal (I_H^V) components of fluorescence intensity excited by vertically polarized light were recorded for determination of fluorescence anisotropy (r). The different sensitivity of the registering system for vertical and horizontal components was taken into account:

$$r = \frac{I_V^V - GI_H^V}{I_V^V + 2GI_H^V} \quad (1)$$

where G is the ratio of vertical and horizontal components of fluorescence intensity excited by horizontally polarized light ($G = I_V^H/I_H^H$).

Circular Dichroism Measurements. Far-UV CD spectra were obtained with a dichrograph Mark V (Jobin-Yvon, USA) in a 0.1 cm path length cell. Actin concentration was 0.4 mg/mL. CD spectra of the appropriate buffers were recorded and subtracted from the protein spectra.

Registration of the Kinetics of Actin Denaturation. All kinetic experiments were performed in micro cells 101.016-QS 5×5 mm (Hellma, Germany). Unfolding of the protein was initiated by manual mixing of the protein solution with buffer containing the corresponding amount of GdnHCl; 350 μL of the GdnHCl solution of appropriate concentration was injected in the cell with 50 μL of the solution of native protein. The dead time was determined from the control experiments. To this end 350 μL of buffer G was injected in the cell with 50 μL of the solution of native protein, and 350 μL of 4.0 M GdnHCl was injected in 50 μL of the solution of protein in the 4.0 M GdnHCl. These experiments showed that the dead time of kinetic measurements was less than 4 s. The final concentration of protein was 0.1–0.01 mg/mL. The character of the kinetic curves and the calculated values of rate constants k_1 , k_2 , and k_3 (see below) were invariant of actin concentration within these limits. The spectrofluorimeter was equipped with thermostat that held a constant temperature of 23 °C in the cell and in the special box where the solutions are held before mixing.

The time courses of changes in the parameter A value were constructed using the experimental kinetic curves of fluorescence intensities successively registered at 320 and 365 nm. The kinetic curves of fluorescence anisotropy (r) were calculated on the basis of the experimental kinetic curves of vertical (I_V^V) and horizontal (I_H^V) components of fluorescence intensity excited by vertically polarized light and registered successively.

RESULTS

To clarify the process of GdnHCl-induced formation of inactivated actin, kinetic curves reflecting the denaturant-induced changes in the intensity of intrinsic fluorescence were studied (see Figure 1A). The dependence of fluorescence intensity on the GdnHCl content after 24 h of incubation under conditions of desired denaturant concentration (Figure 1B) and complete spectra for native (N), inactivated (I), and unfolded (U) actin were registered (Figure 1B insert). Comparison of the fluorescence spectra in native, inactivated, and unfolded states shows that the greatest differences in fluorescence intensity are in the vicinity of 320 nm. That is why the wavelength 320 nm was used for the registration of the kinetic curves. Figure 1A shows that the shapes of the kinetic curves registered at various final GdnHCl concentrations differ significantly.

At low GdnHCl concentrations (below 1.0 M) the fluorescence intensity decreases monotonically with time, slowly approaching its equilibrium values (cf. Figure 1). At high GdnHCl concentrations (above 3.0 M) the intensity of actin intrinsic fluorescence also decreases monotonically and rapidly approaching the value typical of the completely unfolded protein (Figure 1A). The most intriguing results were obtained for moderate GdnHCl concentrations from 1.0 to 2.0 M. Within this concentration range, the fluorescence intensity first decreases over time but then increases slowly to the equilibrium value (Figure 1B).

The GdnHCl-induced change in the position and shape of the fluorescence spectrum over time was also studied. For this purpose, the changes in ratio of the intensities on two slopes of the spectrum, the so-called spectral parameter $A = I_{320}/I_{365}$, were used (47). Figure 2 shows the time course of parameter A measured at 1.2 M GdnHCl. The insert to Figure 2 represents the dependence of the parameter A value on GdnHCl concentration determined after 24 h incubation of the protein at the desired denaturant concentration. It can be seen that early in the unfolding process the position and shape of the fluorescence spectrum tend to be similar to those typical of the completely unfolded protein. Then parameter A slowly increases and finally reaches the equilibrium value observed after 24 h incubation of the protein in the presence of 1.2 M GdnHCl.

Figure 3A shows the time courses of the fluorescence anisotropy changes, accompanying the unfolding of actin at 1.2 and 4.0 M final GdnHCl concentration, while the equilibrium fluorescence anisotropy values are shown in Figure 3B. Kinetic curves were calculated from the experimentally registered time courses of vertical and horizontal components of intrinsic fluorescence (Figure 3A insert).

Registering far-UV CD spectra also monitored the kinetics of actin structural changes induced by GdnHCl. Figure 4 shows the far-UV CD spectra of actin in 1.8 M GdnHCl

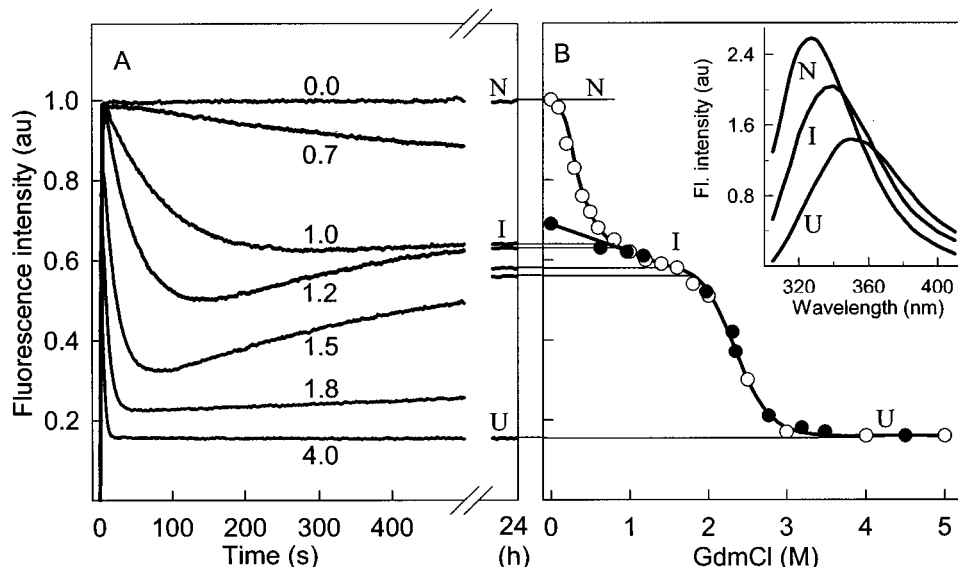


FIGURE 1: Actin denaturation monitored by the change of intrinsic fluorescence intensity at 320 nm. (A) Kinetics of actin denaturation induced by GdnHCl. The values on the curves are the concentration of GdnHCl. (B) Fluorescence intensity of actin recorded after 24 h of incubation in the definite concentrations of GdnHCl. Open and black symbols correspond to the unfolding and refolding experiments, respectively. In the experiment of refolding the appropriate concentration of GdnHCl was obtained by dilution of the actin solution in 5 M GdnHCl. Protein concentration was 0.1 mg/mL, $\lambda_{\text{ex}} = 297$ nm, and $\lambda_{\text{em}} = 320$ nm. Insert: Fluorescence spectra of native (N), inactivated (I), and completely unfolded (U) actin.

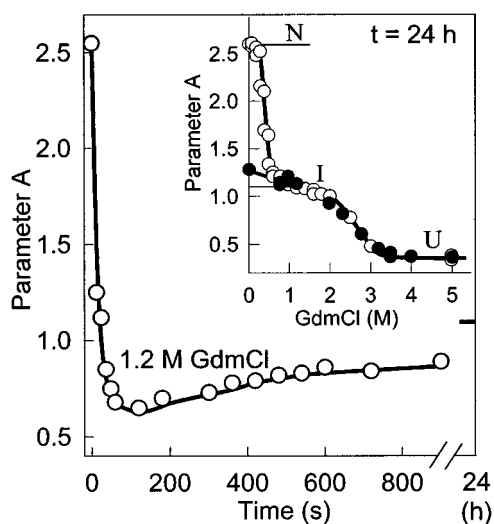


FIGURE 2: Kinetics of actin denaturation monitored by the change of parameter $A = I_{320}/I_{365}$. The final concentration of GdnHCl is 1.2 M. Insert: Parameter A of actin in the definite concentrations of GdnHCl recorded after 24 h of incubation and $\lambda_{\text{ex}} = 297$ nm. Open and black symbols correspond to the unfolding and refolding experiments, respectively.

measured just after mixing native actin with GdnHCl solution and overnight.

DISCUSSION

In all studies devoted to actin unfolding it has been assumed that actin successively transfers from native to inactivated and then to the completely unfolded state (29–41):



i.e., inactivated actin (I) was considered as an on-pathway intermediate between the native (N) and completely unfolded (U) states. All equilibrium experiments appeared to support this model. In fact, data presented in Figures 1B and 3B and

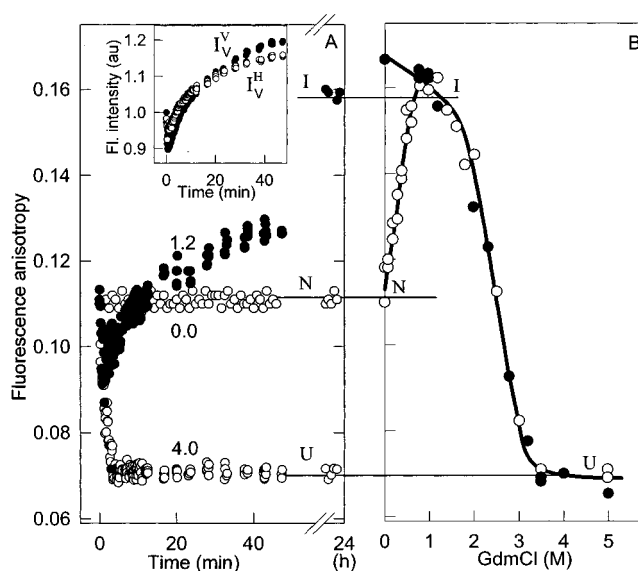


FIGURE 3: Actin denaturation monitored by the change of intrinsic fluorescence anisotropy. (A) Kinetics of actin denaturation induced by GdnHCl. The values on the curves are the concentration of GdnHCl. Insert: Kinetics of actin denaturation monitored by the change of vertical (I_V^V) and horizontal (I_V^H) components of fluorescence intensity of intrinsic actin fluorescence. The final concentration of GdnHCl is 1.2 M. (B) Fluorescence anisotropy of actin in the definite concentrations of GdnHCl recorded after 24 h of incubation. Open and black symbols correspond to the unfolding and refolding experiments, respectively. Protein concentration was 0.1 mg/mL, $\lambda_{\text{ex}} = 297$ nm, and $\lambda_{\text{em}} = 365$ nm.

in the insert to Figure 2 suggest that GdnHCl induces two successive conformational transitions in actin. The transition from native to inactivated actin takes place at low GdnHCl concentrations (0.0–0.8 M), whereas the transformation of the inactivated actin into completely unfolded protein occurs between 1.8 and 4.0 M GdnHCl. It also suggests that in the relatively wide range of GdnHCl concentrations, between 0.8 and 1.8 M, actin exist in its inactivated form.

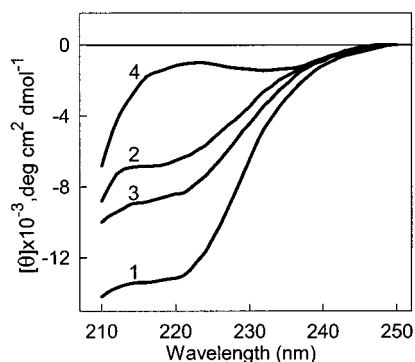


FIGURE 4: Far-UV-CD spectrum of G-actin in different conformational states: 1, native protein; 2 and 3, actin at 1.8 M GdnHCl recorded immediately after addition of GdnHCl (1 min) and after 24 h of incubation, respectively; 4, unfolded actin (6.0 M GdnHCl). All measurements were carried out at a protein concentration of 0.4 mg/mL and a cell path length of 0.1 cm.

Finally, it is necessary to emphasize that the transition from the native to the inactivated state is irreversible (30, 39–42). Thus, all structural characteristics of actin in the region of low denaturant concentration (from 0 to 0.8 M GdnHCl) are quasi-stationary. In this regard it should be noted that the curves in Figure 1B, Figure 2 (insert), and Figure 3B were recorded after 24 h incubation of the actin in solution with the desired GdnHCl concentration. Irreversibility of the $N \rightarrow I$ transition demands the kinetic investigations of the inactivated actin formation.

New Kinetic Scheme of Actin Unfolding. The minimum seen in the kinetic curves at 1.0, 1.2, 1.5, and 1.8 M GdnHCl suggests that the transition from the native to the inactivated state occurs via some intermediate state in which the fluorescence intensity is lower than in the native and the inactivated state (Figure 1A). It is known that actin in the completely unfolded state has the lowest intensity at 320 nm compared to native and inactivated actin (Figure 1B). Thus it was suggested that inactivated actin is formed from native actin via essentially unfolded state.

Same shape of the kinetic curves was found when changes in other spectroscopic characteristics were analyzed. In this respect we studied the parameters for which values for unfolded actin were lower than those for the native and inactivated states and which in contrast to fluorescence intensity defined the structure of the protein qualitatively. Kinetic curves measured at 1.0–2.0 M GdnHCl for parameter $A = I_{320}/I_{365}$ (that reflects the fluorescence spectrum position and shape) (Figure 2) and fluorescence anisotropy (Figure 3A) were also characterized by a specific minimum. It is known that the value of fluorescence anisotropy decreases with the increase in the mobility of the chromophore. Thus, association of the protein molecules is usually accompanied by the anisotropy increase, whereas dissociation of oligomers and unfolding of the protein result in the anisotropy decrease. In agreement with these conclusions, Figure 3B shows that the formation of inactivated actin [which was shown to be a 15-mer (42, 43)] is accompanied by an essential increase in the fluorescence anisotropy. On the other hand, the unfolding of protein is characterized by pronounced drop in the anisotropy value (see Figure 3B). As it was exposed, Figure 3A shows that the kinetic curve of fluorescence anisotropy at moderate GdnHCl concentra-

tion (1.2 M) has a minimum. This means that actin essentially unfolds prior the appearance of the inactivated conformation. Importantly, with time the values of parameter A and fluorescence anisotropy were approaching the values typical for inactivated actin (Figures 2 and 3).

Furthermore, the far-UV CD spectrum of actin measured immediately after the addition of GdnHCl to a final concentration of 1.8 M was between that of the completely unfolded and the inactivated protein, whereas further incubation in the presence of denaturant (for 24 h) led to the CD spectrum typical of the inactivated actin (Figure 4). At the same time it is necessary to mention that this essentially unfolded state, which precedes the inactivated state, preserves pronounced secondary structure. So the properties of this state resemble that of the molten globule state.

On the basis of all experimental data, the following scheme of actin unfolding was proposed:



where k_i are the constants of the corresponding process and U^* is essentially unfolded kinetic intermediate, whose fluorescence properties are similar to those of the completely unfolded state but whose secondary structure is much more ordered. The transition from U^* to I is most likely to be irreversible. Nonetheless, we regard the more general situation taking into account k_3 . At GdnHCl concentration greater than 1.8 M the scheme must take into account the reversible transition between I and U . In this work this transition is not regarded. In the frame of the kinetic scheme (eq 3) the time dependencies of the protein fraction in native $\alpha_N(t)$, inactivated $\alpha_I(t)$, and essentially unfolded $\alpha_{U^*}(t)$ states are

$$\alpha_N(t) = [N(t)]/[N(0)] = e^{-k_1 t}$$

$$\alpha_{U^*}(t) = [U^*(t)]/[N(0)] = [(-k_2 k_1 + k_3 k_2 - k_3 k_1 + k_3^2) e^{-k_1 t} - k_3 k_2 + k_3 k_1 - k_3^2 + k_2 k_1 e^{-(k_2+k_3)t}] / (k_2 + k_3)(k_1 - k_2 - k_3)$$

$$\alpha_I(t) = [I(t)]/[N(0)] = -k_2(k_1 e^{-(k_2+k_3)t} - (k_1 + k_2) e^{-k_1 t} - k_1 + k_2 + k_3) / (k_2 + k_3)(k_1 - k_2 - k_3) \quad (4)$$

The fitting routine to analyze the kinetic curves of the relative fluorescent intensity and to determine the rate constants k_i and the fraction of the protein in the native, inactivated, and essentially unfolded states was based on the nonlinear least-squares method.

Analysis of the Actin Unfolding Kinetics. The time dependence of fluorescence intensity of the system containing actin in the native, inactivated, and essentially unfolded state is determined by the equation:

$$I(t) = \alpha_N(t)I_N + \alpha_I(t)I_I + \alpha_{U^*}(t)I_{U^*} \quad (5)$$

where $\alpha_N(t)$, $\alpha_I(t)$, and $\alpha_{U^*}(t)$ are the fraction of the protein in the native, inactivated, and essentially unfolded kinetic intermediate states; I_N , I_I , and I_{U^*} are fluorescence intensities of actin in these states, respectively; and $\alpha_N(t) + \alpha_{U^*}(t) +$

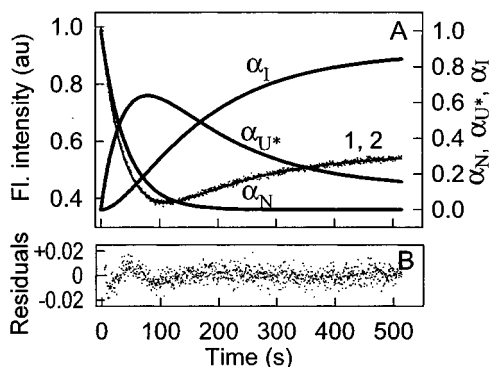


FIGURE 5: Analysis of the kinetic curves of actin denaturation monitored by the change of intrinsic fluorescence intensity. The final concentration of GdnHCl is 1.2 M. $\lambda_{\text{ex}} = 297$ nm, and $\lambda_{\text{reg}} = 320$ nm. (A) Curves 1 and 2: experimental decay curve (points) and the calculated best fit of the fluorescence intensity that corresponds to the values $k_1 = 2.1 \times 10^{-2}$, $k_2 = 7.2 \times 10^{-3}$, and $k_3 = 7.6 \times 10^{-4} \text{ s}^{-1}$, respectively. Curves α_N , α_I , and α_{U^*} : changes of the fractions of the actin molecule in native, inactivated, and unfolded states, respectively. The values of k_i and curves α_N , α_I , and α_{U^*} were calculated on basis of the kinetic scheme (eq 3) and eqs 4–7. (B) Deviation between the experimental and calculated curves.

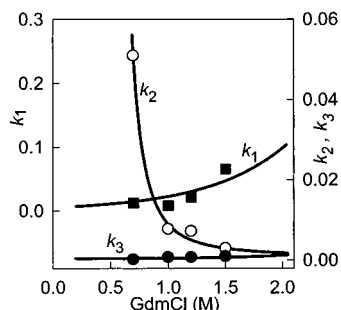


FIGURE 6: Dependencies of the rate constants of actin denaturation k_i from GdnHCl concentration.

$\alpha_I(t) = 1$. Excluding $\alpha_N(t)$ and assuming that $I_{U^*} = I_U$, we have

$$I_r(t) = 1 + \alpha_I(t)(I_U/I_N - 1) + \alpha_{U^*}(t)(I_U/I_N - 1) \quad (6)$$

where $I_r(t) = I(t)/I(0)$ is the relative fluorescent intensity, $I(0) = I_N$. The particular relation of $\alpha_N(t)$, $\alpha_I(t)$, and $\alpha_{U^*}(t)$ with the rate constants k_i is determined by the concrete kinetic scheme that fits the unfolding process (see above). The values of rate constants k_i were determined on the basis of the experimental kinetic curves, reflecting changes in fluorescence intensities, by the nonlinear least-squares method, as the values that fit the minimum of the sum of the squares of the residuals:

$$\Phi = \sum_t [I_{r,0}(t) - I_r(\alpha_j(t, k_i))]^2 \quad (7)$$

In this expression $I_{r,0}(t)$ and $I_r(\alpha_j(t, k_i))$ are experimental and calculated values of the relative intensity. The fitting was done according to Marquardt (48).

As an example Figure 5 shows the experimental kinetic curve, which reflects the time course of changes in fluorescence intensity and the best theoretical fit within the frame of the model (eq 3), both for the final GdnHCl concentration of 1.2 M. The best fit of the experimental data was achieved when $k_1 = 2.1 \times 10^{-2}$, $k_2 = 7.2 \times 10^{-3}$, and $k_3 = 7.6 \times$

10^{-4} s^{-1} . This figure represents also the changes in the populations of native (α_N), inactivated (α_I), and essentially unfolded (α_{U^*}) actin molecules, calculated according to eq 4. Figure 5B shows that the residuals are of statistical character, though there is a small nonlinearity for short times. The proximity of chi square [$\chi^2 = \Phi/(n - p)$, where n is the number of experimental points and p is the number of examined parameters] to the unity ($\chi^2 = 1.12$) and the randomness of the residuals prove the validity of the chosen kinetic model.

GdnHCl Dependence of the Rate Constants k_i . The GdnHCl dependencies of the rate constants k_1 , k_2 , and k_3 were determined (Figure 6). As one would expect, k_3 is practically equal to zero. At small denaturant concentration k_2 is considerably greater than k_1 . Therefore, the limiting stage of the reaction under these conditions is protein unfolding, whereas all unfolded molecules will immediately refold to form the inactivated actin. With the increase in GdnHCl concentration the rate constant k_1 increased and the rate constant k_2 decreased. This leads to the accumulation of essentially unfolded molecules early in the unfolding process (in the range of 1.0–2.0 M GdnHCl) and, consequently, to the appearance of the characteristic minimum in the kinetic curves (Figures 1–3).

Thus, our data show that inactivated actin does not represent an intermediate state in the pathway of this protein unfolding from the native to the unfolded state, as has been suggested earlier. On the contrary, this conformation should be considered as an off-pathway species, which appears via the primary unfolding of the protein. This result may be also essential for the search of the pathways of actin folding in vitro.

ACKNOWLEDGMENT

We are very grateful to Prof. A. L. Fink and Dr. V. N. Uversky for valuable discussions. V. V. Verkhusha thanks S. Tsukita and the JST Corp. for the possibility to do part of this work while participating in the Tsukita Cell Axis Project, Japan.

REFERENCES

- De Young, L. R., Fink, A. L., and Dill, K. (1993) *Acc. Chem. Res.* 26, 614–620.
- De Young, L. R., Dill, K., and Fink, A. L. (1993) *Biochemistry* 32, 3877–3886.
- Oberg, K., Chrnyk, B. A., Wetzel, R., and Fink, A. L. (1994) *Biochemistry* 33, 2628–2634.
- Fink, A. L. (1995) *Methods Mol. Biol.* 40, 343–360.
- Fink, A. L. (1995) *Annu. Rev. Biophys. Biomol. Struct.* 24, 495–522.
- Semisotnov, G. V., Kihara, H., Kotova, N. V., Kimura, K., Amemiya, Y., Wakabayashi, K., Serdyuk, I. N., Timchenko, A. A., Chiba, K., Nikaido, K., Ikura, T., and Kuwajima, K. (1996) *J. Mol. Biol.* 262, 559–574.
- Fink, A. L. (1998) *Folding Des.* 3, R9–R23.
- Uversky, V. N., Segel, D. J., Doniach, S., and Fink, A. L. (1998) *Proc. Natl. Acad. Sci. U.S.A.* 95, 5480–5483.
- Marston, F. A. (1986) *Biochem. J.* 240, 1–12.
- Schein, C. H. (1989) *Bio/Technology* 7, 1141–1149.
- Frankel, S., Condeelis, J., and Leinwand, L. (1990) *J. Biol. Chem.* 265, 17980–17987.
- Wetzel, R. (1992) in *Protein Engineering. A Practical Approach* (Rees, A. R., Sternberg, A. R., and Wetzel, R., Eds.) pp 191–219, IRL Press, Oxford.

13. Wetzel, R. (1992) in *Stability of Protein Pharmaceuticals, Part B: In Vivo Pathways of Degradation and Strategies for Protein Stabilization* (Ahern, T. J., and Manning, M. C., Eds.) Vol. 3, pp 43–88, Plenum Press, New York.
14. Wetzel, R. (1994) *Trends Biotechnol.* 12, 193–198.
15. Speed, M. A., Wang, D. I., and King, J. (1996) *Nat. Biotechnol.* 14, 1283–1287.
16. Massry, S., and Glasscock, R. (1983) *Textbook of Nephrology*, Williams and Wilkins, Baltimore, MD.
17. Carrell, R. W., and Gooptu, B. (1998) *Curr. Opin. Struct. Biol.* 8, 799–809.
18. Clark, J., and Steele, J. (1992) *Proc. Natl. Acad. Sci. U.S.A.* 89, 720–1722.
19. Kelly, J. W. (1997) *Structure* 5, 595–600.
20. Harper, J. D., and Lansbury, P. T., Jr. (1997) *Annu. Rev. Biochem.* 66, 385–407.
21. Koo, E. H., Lansbury, P. T., Jr., and Kelly, J. W. (1999) *Proc. Natl. Acad. Sci. U.S.A.* 96, 9989–9990.
22. Lansbury, P. T., Jr. (1999) *Proc. Natl. Acad. Sci. U.S.A.* 96, 3342–3344.
23. Hashimoto, M., and Masliah, E. (1999) *Brain Pathol.* 9, 707–720.
24. Uversky, V. N., Talapatra, A., Gillespie, J. R., and Fink, A. L. (1999) *Med. Sci. Monit.* 5, 1001–1012.
25. Uversky, V. N., Talapatra, A., Gillespie, J. R., and Fink, A. L. (1999) *Med. Sci. Monit.* 5, 1238–1254.
26. Kabsch, W., Mannherz, H. G., Suck, D., Pai, E. F., and Holms, H. C. (1990) *Nature* 347, 37–44.
27. Kuznetsova, I. M., Yakusheva, T. A., and Turoverov, K. K. (1999) *FEBS Lett.* 452, 205–210.
28. Doyle, T. C., Hansen, J. E., and Reisler, E. (2001) *Biophys. J.* 80, 427–434.
29. Lehrer, S. L., and Kerwar, G. (1972) *Biochemistry* 11, 1211–1217.
30. Turoverov, K. K., Bictashev, A. G., Khaitlina, S. Yu., and Kuznetsova, I. M. (1999) *Biochemistry* 38, 6261–6269.
31. Strzelecka-Golaszewska, H., Venyaminov, S. Yu., Zmorzynski, S., and Mossakowska, M. (1985) *Eur. J. Biochem.* 147, 331–342.
32. Nagy, B., and Jencks, W. P. (1962) *Biochemistry* 1, 987–996.
33. West, J. J., Nagy, B., and Gergely, J. (1967) *J. Biol. Chem.* 242, 1140–1145.
34. Nagy, B., and Strzelecka-Golaszewska, H. (1972) *Arch. Biochem. Biophys.* 150, 428–435.
35. Strzelecka-Golaszewska, H., Nagy, B., and Gergely, J. (1974) *Arch. Biochem. Biophys.* 161, 559–569.
36. Contaxis, C. C., Bigelow, C. C., and Zarkadas, C. G. (1977) *Can. J. Biochem.* 55, 325–331.
37. Tatumashvili, L. V., and Privalov, P. L. (1984) *Biofizika* 29, 583–585.
38. Kuznetsova, I. M., Khaitlina, S. Yu., Konditerov, S. N., Surin, A. M., and Turoverov, K. K. (1988) *Biophys. Chem.* 32, 73–78.
39. Bertazzon, A., Tian, G. H., Lamblin, A., and Tsong, T. Y. (1990) *Biochemistry* 29, 291–298.
40. Le Bihan, T., and Gicquaud, C. (1993) *Biochem. Biophys. Res. Commun.* 194, 1065–1073.
41. Schuler, H., Lindberg, U., Schutt, C. E., and Karlsson, R. (2000) *Eur. J. Biochem.* 267, 476–486.
42. Kuznetsova, I. M., Biktashev, A. G., Khaitlina, S. Yu., Vassilenko, K. S., Turoverov, K. K., and Uversky, V. N. (1999) *Biophys. J.* 77, 2788–2800.
43. Kuznetsova, I. M., Turoverov, K. K., and Uversky, V. N. (1999) *Protein Pept. Lett.* 6, 173–178.
44. Pardee, J. D., and Spudich, J. A. (1982) *Methods Enzymol.* 85B, 164–181.
45. Turoverov, K. K., Khaitlina, S. Yu., and Pinaev, G. P. (1976) *FEBS Lett.* 62, 4–7.
46. Rees, M. K., and Young, M. (1967) *J. Biol. Chem.* 242, 4449–4458.
47. Turoverov, K. K., Biktashev, A. G., Dorofeyuk, A. S., and Kuznetsova, I. M. (1998) *Tsitologiya* 40, 806–817.
48. Marquardt, D. W. (1963) *J. Soc. Ind. Appl. Math.* 11, 431–441.

BI015548C